REVSTAT – Statistical Journal
Volume 22, Number 1, January 2024, 45–60
https://doi.org/10.57805/revstat.v22i1.454

Tales of the Wakeby Tail and Alternatives when Modelling Extreme Floods

Author: Jesper Rydén
– Department of Energy and Technology, Swedish University of Agricultural Sciences, Uppsala, Sweden
jesper.ryden@slu.se

Received: March 2020 Revised: January 2022 Accepted: January 2022

Abstract:

- Estimation of return levels, based on extreme-value distributions, is of importance in the earth and environmental sciences. The selection of an appropriate probability distribution is crucial. The Wakeby distribution has shown to be an interesting alternative. By simulation studies, we investigate by various means of minimum distance to distinguish between common distributions when modelling extreme events in hydrology. Estimation of parameters is performed by L-moments. Moreover, time series of annual maximum floods from major unregulated rivers in Northern Sweden were analysed with respect to fitting an appropriate distribution. The results of the simulation study shows that the Wakeby distribution has the best fit of the tail for a wide range of sample sizes. For the analysis of extreme floods, the Wakeby distribution is in the majority of cases the best fit by means of minimum distance. However, when considering estimation of return levels by competing distributions, results can vary considerably for longer return periods.

Keywords:

- *Wakeby distribution; GEV distribution; L-moments; distance measures; floods.*

AMS Subject Classification:

- 62G32, 62P12.

1. INTRODUCTION

In the earth sciences, statistical modelling of extreme events is of importance; in fields like hydrology and oceanography there is a need to estimate return levels, for instance for the sake of engineering design. For this purpose, quantiles of probability distributions are of key interest, and hence choice of distribution is crucial. When using statistical methodology based on likelihood functions, criteria like Akaike's Information Criterion (AIC) and Bayesian Information Criterion (BIC) can be employed for model choice [2], [25]. Often in the applied literature, goodness-of-fit tests are employed as measures of deviation between the empirical distribution and the potential distribution family.

The tail behaviour of the probability distribution is a key factor in extreme-value analysis, e.g. when estimating return levels. When a block-maximum approach is chosen for studying annual maxima of some quantity (e.g. daily maximum rainfall), extreme-value theory tells that certain distributions serve as limiting distributions, that can be summarised in the Generalised Extreme Value (GEV) distribution. However, the results are valid asymptotically and not seldom only small samples are available. In hydrology, one occasionally also considers the lognormal distribution and other alternatives, like the five-parameter Wakeby distribution, first presented in 1978 by Houghton [16] and to be investigated more closely in the sequel of this paper. Griffiths [10] claims that "the distribution has a secure theoretical basis and is hydrologically more realistic". A list of applications of this distribution is given in a recent paper by Busababodhin *et al.* along with proposed estimation techniques [7].

In recent years, generalisations of conventional distributions have been introduced, with the intention of being more flexible. Exponentiated distributions have for instance been proposed: exponentiated exponential, exponentiated Gumbel etc. For an investigation of the exponentiated Gumbel applied to series of significant wave height, see Persson and Rydén [23]. Another generalisation of the Gumbel distribution, the so-called Beta Gumbel distribution, was studied by Jonsson and Rydén [17], where this distribution was compared to the Gumbel and GEV distributions in a case study of extreme precipitation. However, for that study the difference between Beta Gumbel and GEV was minor, with respect to infomation criteria as well as estimated return levels and their uncertainties.

This paper serves two purposes. First, to check the intended flexibility of the Wakeby distribution through simulation studies for various sample sizes. Estimation of parameters will be made conveniently by L-moments [13], and hence the likelihood-based AIC and BIC are not options for model choice. Examinations of the differences between simulated samples and candidate distributions are based on various measures of minimum distance. As the tail behaviour is of particular interest for typical applications, upper quantiles are also compared. The second purpose is to study data of unregulated extreme floods in northern Sweden. Several distributions are considered, in particular the effects on estimated return levels due to various distribution assumptions on the tails. Moreover, the influence of record length is of interest.

The paper is outlined as follows. Section 2 serves as a background, introducing first of all the Wakeby distribution. Further, a review of the methodology for estimation by L-moments is given as well as presentation of the approaches for discerning distributions.

The simulation study is outlined and its main findings given in Section 3, and in Section 4 the case study of extreme floods in Sweden is presented, including estimated return levels for various situations.

2. BACKGROUND

2.1. The Wakeby distribution with applications

The Wakeby distribution was presented by Houghton [16], along with results of goodness-of-fit tests for observations of extreme floods. We here give the parametrisation by Hosking and Wallis found in [15], a five-parameter distribution:

$$x(F) = \xi + \frac{\alpha}{\beta}\left[1 - (1-F)^{\beta}\right] - \frac{\gamma}{\delta}\left[1 - (1-F)^{-\delta}\right], \tag{2.1}$$

where $F \in [0, 1]$. The following parameter restrictions are valid: either $\beta + \delta > 0$ or $\beta = \gamma = \delta = 0$; if $\alpha = 0$ then $\beta = 0$; if $\gamma = 0$ then $\delta = 0$. The generalised Pareto distribution follows with the formulation in equation (2.1) as the special $\alpha = 0$ or $\gamma = 0$. Note that the definition is stated in terms of the quantile function, which faciliates estimation of return levels. In addition, simulation of random numbers can be performed by the inverse method.

This distribution has been applied successfully for various quantities in the earth sciences. A list of applications is given in [7]. In his landmark paper [16], Houghton examined the fit of observations of floods from stations in the United States, and Griffiths [10] investigated flood data from New Zealand.

2.2. Estimation of parameters

In this study, we employ estimation by L-moments, which is convenient for the five-parameter Wakeby distribution. For instance, Busababodhin *et al.* point out that maximum-likelihood estimates are not easily obtained [7]. Moreover, the methodology is in widespread use in many countries; see [6] for a list of studies performed by L-moments. Hosking [13] claims that estimation of parameters by L-moments is occasionally more accurate in small samples. Furthermore, quantile functions can be expressed in terms of L-moments, a clear advantage in hydrological sciences when estimating return levels. For the computational work in this paper, the implementations in the R packages `lmom` and `lmomco` were used ([14], [5]), following the parameterisation in equation (2.1).

2.2.1. Introduction to L-moments

The methodology with L-moments was introduced by Hosking [13]. The L-moments are the quantities λ_r as follows, and are linear functions of order statistics:

$$\lambda_r = \frac{1}{r}\sum_{k=0}^{r-1}(-1)^k\binom{r-1}{k}\mathsf{E}[X_{r-k:r}], \quad r = 1, 2, ...,$$

where $X_{1:n} \leq \cdots \leq X_{n:n}$ are the order statistics of a random sample of size n drawn from the distribution of a random variable X. In applied studies, moments could be standardised, becoming independent of the units of measurement. These so-called L-moment ratios are the quantities

$$\tau_r = \lambda_r/\lambda_2, \quad r = 3, 4, ... \ .$$

The measures τ_3 and τ_4 can be regarded as measures of skewness and kurtosis. For instance, for a symmetrical distribution, $\tau_3 = 0$. Further details on L-moments are found in Appendix.

2.2.2. Remarks on estimation methodologies

The notion of L-moments has been extended, for instance trimmed L-moments (TL moments), [9]. TL moments with the smallest value trimmed with an application to the generalised Pareto distribution were considered in [1]. An estimation method using higher-order L-moments, so-called LH-moments, was presented in [7].

Recently, versions of L-moments as well as maximum-likelihood methods for estimation of high quantiles of the generalised Pareto and generalised extreme-value distribution have been compared [27]. The authors concluded that "there are small differences when estimating high quantiles of the GPD or GEV distributions. It was revealed that L-moment and maximum likelihood methods outperform LQ- and TL-moment methods: the L-moment method is preferred for heavy-tailed distributions, while the maximum likelihood method is recommended for light-tailed distributions." Thus, from these findings, we are motivated in the choice of estimation by L-moments in this paper.

2.3. Evaluating candidate distributions

Already in the paper by Houghton [16], goodness-of-fit tests were considered in the analysis, and many papers in e.g. hydrology apply various versions of such tests. However, as pointed out by Wilks [28]: "Of substantially more interest is the closeness of fit on the right tail, since it is here that extrapolations of relevance to engineering design and other applications will be made." In the literature, there seems to be no concensus on a specific procedure (in the forms of visualisations, goodness-of-fit measures, computer-intensive methods) to apply. Uses of criteria like AIC and BIC for model choice is often a convenient strategy, not the least to compare distributions (or models) with varying number of parameters.

However, in this paper we use L-moments for estimation, not maximum-likelihood estimation, and hence other approaches have to be taken.

In the sequel of this paper, we will perform simulations from a particular distribution and compare to candidate distributions (to be described in detail in Section 3). The so resulting samples will be compared by firstly, two general distance measures, secondly, comparison of high quantiles. Moreover, when analysing observed river-flow data from stations in Section 4, the so-called L-moment diagram will assist in interpretations.

2.3.1. Distance measures

In the literature, there is a substantial number of distance, or similarity, measures in various scientific fields. A review is given by Cha, where measures also are categorised [8]. In the presentation below, we assume that two probability densities P and Q, each in a discretised "histogram" form of B values, are to be compared.

Some measures are said to belong to Shannon's entropy family. In this paper, we chose the Kullback–Leibler distance [18]:

$$d_{\mathrm{KL}} = \sum_{j=1}^{B} p_i \ln \frac{p_i}{q_i}.$$

In another category, the measures are based on geometric means: the fidelity or squared-chord family. The simplest version was chosen in this paper, the Fidelity similarity measure:

$$s_{\mathrm{F}} = \sum_{j=1}^{B} \sqrt{p_j q_j}.$$

Other alternatives in this category are Bhattacharyya and Hellinger distances. Both d_{KL} and s_{F} are interpreted that the smaller the value, the two objects (here, distributions) are closer and have a higher degree of similarity.

2.3.2. Comparison of quantiles

For a simulated sample from a specified random variable X, the upper quantile $x_{0.99}$ for which $\mathsf{P}(X > x_{0.99}) = 0.01$, is estimated, resulting in $x^*_{0.99}$, say. Based on the simulated sample, candidate distributions are fitted with L moments, and the related upper quantiles are estimated. The absolute differences between these estimates and $x^*_{0.99}$ are finally calculated. Further details on the simulation procedure are given in Section 3.1.

3. SIMULATION STUDY: DIFFERENCES AMONG DISTRIBUTIONS

In this section, we investigate how distances between distributions differ, given simulated observations from a parent distribution. We will use the approaches presented in Section 2.3. In addition to the Wakeby distribution, we will consider two other distributions

often encountered in the earth sciences or hydrology: the generalised extreme value (GEV) distribution and the three-parameter lognormal (LN3). Though familiar and well known in the research domains mentioned, we present them below in order to present their parameters.

The GEV distribution has three parameters (location μ, scale σ and shape ξ), and is commonly stated by its distribution function:

$$F(x;\mu,\sigma,\xi) = \begin{cases} \exp\Big\{-\big[1+\xi\frac{x-\mu}{\sigma}\big]^{-1/\xi}\Big\}, & \xi \neq 0, \\ \exp\big\{-\exp\big[-\frac{x-\mu}{\sigma}\big]\big\}, & \xi = 0, \end{cases}$$

where $\mu \in \mathbb{R}$, $\sigma > 0$ and $\xi \in \mathbb{R}$. The shape parameter ξ affects the support of this distribution: when $\xi = 0$, the GEV distribution is the Gumbel distribution (with support $\mathbb{R}$). When $\xi > 0$, the distribution corresponds to the Fréchet distribution with support $x \geq \mu + \sigma/\xi$, and when $\xi < 0$ it corresponds to the reversed Weibull distribution with support $x \leq \mu - \sigma/\xi$.

Consider the LN3 distribution with distribution function

$$F(x) = \Phi(y), \quad x > 0,$$

where $y = (\ln(x-\zeta) - \mu)/\sigma$ and $\Phi(y)$ is the distribution function of the standard normal distribution. In other words, the density function of X is given as

$$f(x;\mu,\sigma,\zeta) = \frac{1}{(x-\zeta)\sigma\sqrt{2\pi}} \exp\left\{-\frac{(\ln(x-\zeta)-\mu)^2}{2\sigma^2}\right\}, \quad x > \zeta \geq 0,$$

where $\mu \in \mathbb{R}$, $\sigma > 0$. If X is distributed as above, $Y = \ln(X-\zeta)$ has a normal distribution with mean μ and variance σ^2.

3.1. Algorithm of simulation study

In this study, we simulate from a given parent distribution: GEV or LN3. The sample size n was chosen in the range from 25 to 200, in steps of 25 at the lower sample sizes.

1. For each sample size, simulate $N = 5000$ samples from a parent distribution.
2. For each sample, compute the L-moments by the R package `lmomco` and then the probability-density functions for the candidate distributions LN3, Wakeby and GEV, evaluated at the sample points.
3. Estimate the probability-density function for the sample (by the R routine `density`), and compute measures s_{F} and d_{KL} for comparison with the densities obtained in step 2. In addition, compute the upper 0.99 quantiles for the sample and the candidate distributions.
4. Register which distribution alternative had the smallest deviation from the simulated sample, in terms of s_{F}, d_{KL} and upper quantile, respectively. Over the N samples the overall proportions of "winners" (in terms of smallest distance) from the three distribution alternatives can be collected, resulting in a triple with the three components summing up to one. For instance, with d_{KL} considered, GEV, LN3 and Wakeby could result in the triple (0.25, 0.15, 0.60), i.e. Wakeby here resulted in the smallest distance in the majority of cases.

3.2. L-moment ratio diagram

Before turning to the simulations outlined above, let us illustrate the notion of the so-called L-moment ratio diagram with simulations from a GEV distribution. In such a diagram is found τ_3 on the abscissa and τ_4 on the ordinate. Probability distributions can be illustrated as curves and in some cases as points. For instance, the uniform distribution has $(\tau_3, \tau_4) = (0, 0)$, for the Gumbel distribution $(\tau_3, \tau_4) \doteq (0.17, 0.15)$, and the GEV distribution forms a curve in the τ_3-τ_4 plane [13].

In Figure 1, the curve for the GEV distribution is drawn along with dots corresponding to L-moments from 500 simulated samples from a GEV distribution. The left panel shows the result for sample size $n = 25$, the right panel shows the case $n = 100$. We note for the smaller sample size a considerable spreading in the (τ_3, τ_4) plane, relatively the larger sample size. This feature could be kept in mind, when facing real data in Section 4.

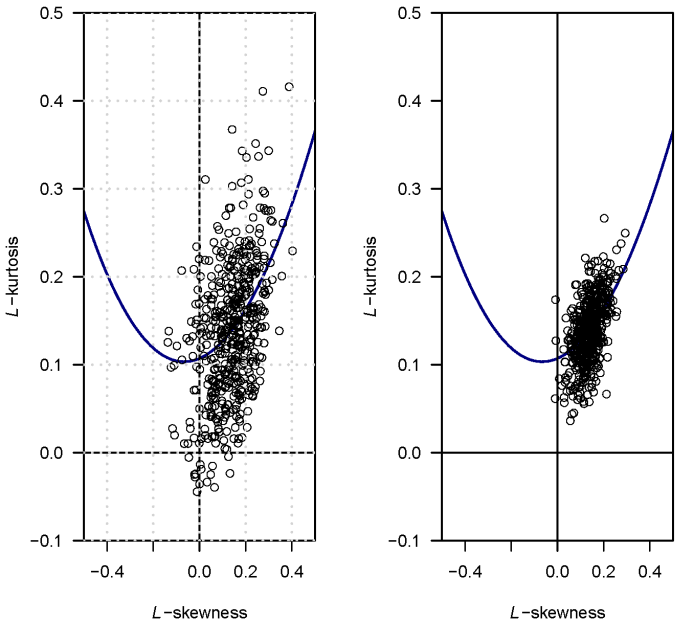

Figure 1: Simulation from a GEV distribution with $\tau_3 = \tau_4 = 0.14$. The solid curve represents a GEV distribution in the (τ_3, τ_4) space. Left panel: sample size 25 (500 samples). Right panel: sample size 100 (500 samples).

An illustration how this type of plot can assist in distinguishing between distributions is found in [13], Section 3.5. This visualisation tecnique has shown itself useful in hydrology [22], [20].

3.3. Case 1. Simulation from GEV distribution

We first study the case of the parent distribution being the standard Gumbel distribution:

$$F(x) = \exp(-\mathrm{e}^{-x}), \quad x \in \mathbb{R}.$$

In Figure 2, the proportions of smallest distance are shown for the three potential distributions as function of sample size. Thus, for each sample size, the proportions obviously sum to one. The left panel shows results based on distance in upper quantile, middle panel d_{KL} and right panel s_{F}.

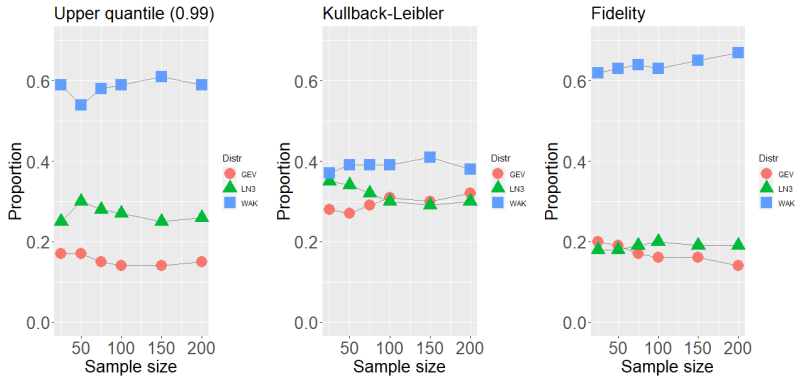

Figure 2: Simulation from a Gumbel distribution ($\tau_3 = 0.17$, $\tau_4 = 0.15$). For each sample size, the proportions of smallest distance for each distribution family are displayed.

From the plots in Figure 2, the Wakeby distribution is for all the measures considered, and regardless of the sample size, the choice which for a majority of cases is the closest to the simulated sample.

In the next example, a GEV distribution with $\tau_3 = 0.07$, $\tau_4 = 0.25$ is the parent distribution, and results are shown in Figure 3. The conclusions are similar to the preceding case: the Wakeby gives in the majority of cases the best fit of the simulated data.

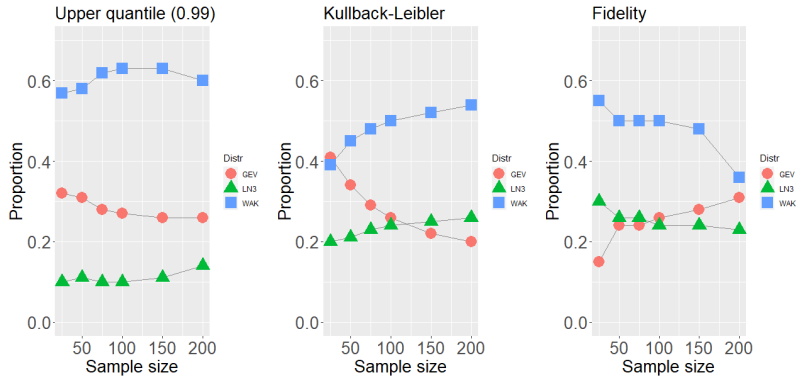

Figure 3: Simulation from a GEV distribution ($\tau_3 = 0.07$, $\tau_4 = 0.25$). For each sample size, the proportions of smallest distance for each distribution family are displayed.

3.4. Case 2. Simulation from log-normal distribution (LN3)

We here simulate from the LN3 distribution with $\tau_3 = 0.07$, $\tau_4 = 0.25$. Results for the three measures are shown in Figure 4. Again, the Wakeby distribution is the best option, regardless of sample size or measure.

Remark. Note that the GEV and LN3 simulations had the same choices of τ_3 and τ_4, respectively. Actually, in order to have realistic values, Station 11 in the next section was used here: fitting each distribution in case by L-moments and rendering parameters in the relevant distribution for the actual simulation study. Obviously, the estimates of τ_3 and τ_4 remain the same, since the same original sample is considered.

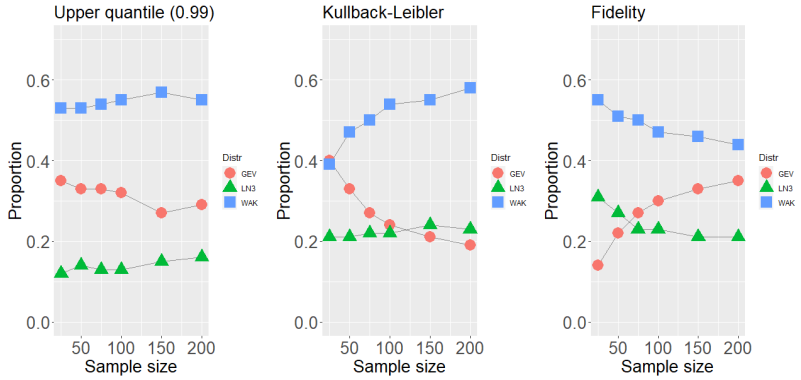

Figure 4: Simulation from an LN3 distribution ($\tau_3 = 0.07$, $\tau_4 = 0.25$). For each sample size, the proportions of smallest distance for each distribution family are displayed.

4. CASE STUDY: FLOOD FLOWS IN SWEDEN

In this section we focus on flood flows from northern Sweden. The aim is to fit annual maximum flows by the three distributions considered earlier in the paper (GEV, LN3, Wakeby). We do not consider possible non-stationary effects due to climate change; for further discussion, see [4], where no significant trends were discerned in annual maximum daily flow in Sweden over the past 100 years.

Data are available from Swedish Meteorological and Hydrological Institute (SMHI), online address: `http://vattenwebb.smhi.se/station/#`. Unregulated rivers in northern Sweden were considered. As long series as possible were chosen, for possible GEV asymptotics to work. In all, eleven stations were selected and descriptions are given in Table 1. For the rest of the paper, they will for simplicity be referred to as Station 1, ..., Station 11.

Table 1: Information on selected stations.

Nr.	Station	Name	River ID	River	Area (km^2)	Start	End
1	4	Junosuando	1000	Torne	4348.0	1968	2019
2	957	Övre Abiskojokk	1000	Torne	566.3	1986	2019
3	2012	Pajala pumphus	1000	Torne	11038.1	1970	2019
4	2357	Abisko	1000	Torneträsk	3345.5	1985	2019
5	2395	Kallio 2	1000	Muonio älv	14477.1	1988	2019
6	16722	Kukkolankoski övre	1000	Torne	33929.6	1911	2019
7	11	Männikkö	4000	Tärendö	5856.2	1976	2019
8	17	Räktfors	4000	Kalix	23102.9	1937	2019
9	1456	Kaalasjärvi	4000	Kalix	1472.5	1975	2019
10	2159	Killingi	4000	Kalix	2345.5	1976	2019
11	2358	Tärendö 2	4000	Kalix	13000.0	1985	2019

For these stations, the L-moments were estimated for each time series, and the results are shown in an L-moment diagram (Figure 5). One could note that stations 7, 9, 10 and 11 tend to form a group in the plane. Indeed, these stations belong to the same river system (Kalix, River ID 4000). Moreover, Stations 2, 4 and 6 are located close to the curve for GEV distribution.

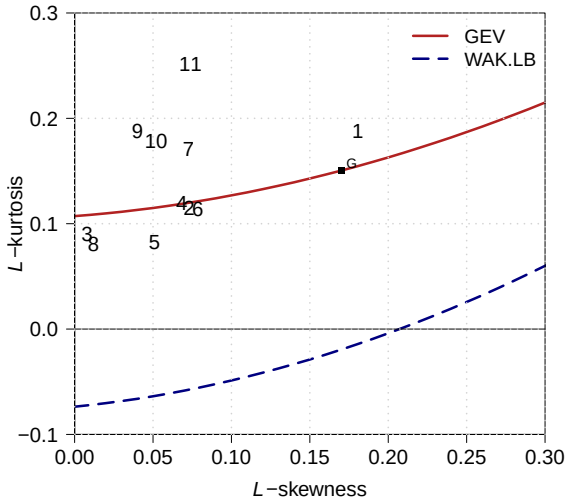

Figure 5: L-moment ratio diagram. Solid line: GEV distribution. Dashed line: Wakeby distribution, lower bound. Numbers: Stations 1–11.

4.1. Estimated quantities

The measures d_{KL} and s_{F} were computed, comparing the original sample and the three candidate distributions with parameters fitted by L-moments. These measures are presented in Table 2 along with estimates of τ_3, τ_4 and the shape parameter ξ in the GEV distribution.

Table 2: Stations 1–11: Estimates of L-moment ratios τ_3 and τ_4; estimate of shape parameter ξ in GEV; distance measures d_{KL} and s_{F} respectively, between sample and fitted candidat distribution.

Station	τ_3	τ_4	Shape ξ	$d_{\mathrm{KL}}^{\mathrm{GEV}}$	$d_{\mathrm{KL}}^{\mathrm{LN3}}$	$d_{\mathrm{KL}}^{\mathrm{WAK}}$	$s_{\mathrm{F}}^{\mathrm{GEV}}$	$s_{\mathrm{F}}^{\mathrm{LN3}}$	$s_{\mathrm{F}}^{\mathrm{WAK}}$
1	0.18	0.19	−0.016	7.304	7.289	7.596	1.765	1.766	1.731
2	0.07	0.12	0.16	13.239	13.262	13.232	2.217	2.215	2.210
3	0.008	0.09	0.27	6.175	6.209	6.130	1.918	1.913	1.926
4	0.07	0.12	0.16	11.667	11.696	11.627	2.269	2.267	2.271
5	0.05	0.08	0.19	12.054	12.077	12.049	2.403	2.397	2.425
6	0.08	0.11	0.15	2.123	2.135	2.091	1.264	1.264	1.264
7	0.07	0.17	0.16	8.862	8.863	9.131	1.949	1.948	1.934
8	0.01	0.08	0.26	2.704	2.690	2.649	1.449	1.446	1.442
9	0.04	0.19	0.21	9.230	9.224	9.039	1.844	1.843	1.825
10	0.05	0.18	0.19	14.759	14.778	15.108	2.062	2.061	2.052
11	0.07	0.25	0.16	11.415	11.417	11.817	1.766	1.765	1.720

From this table, we may reflect upon the following:

- Absolute differences between the measures are generally quite small; the distributions are, in this meaning, close for description of data.
- For each distance measure, d_{KL} and s_{F} respectively, Wakeby gives the closest fit in a majority of cases (7 out of 11 for each measure). For 5 out of 11 samples, *both* measures d_{KL} and s_{F} gave preference for Wakeby.
- Station 6 has the longest period of observations, 109 years. Here one can note that for the measure s_{F}, all three distribution options yield results equal up to the third decimal.
- The GEV distribution is, interestingly, seldom the distribution with minimum distance to the sample. The asympotics of the maximum distribution seems not to have been attained for these samples. From the L-moment ratio diagram in Figure 5, Stations 2, 4 and 6 are close to the GEV curve, but for the measures considered, there are only minor differences between the distribution options.

4.2. Return levels

A T-year return level x_T is often defined as the high quantile for which the probability that the annual maximum exceeds this quantile is $1/T$, hence $F(x_T) = 1 - 1/T$ where $F(.)$ is the distribution function for the series of maxima. We consider T in the range from 10 to 1000 years and estimate return levels based on quantiles for the three distribution families considered above: GEV, LN3, Wakeby.

In Figure 6, we note minor differences between distributions for low T values, but for most stations a considerable spreading for $T = 1000$. In particular, for Stations 2, 9 and 11, the Wakeby 1000-year return level is remarkably higher than the alternatives. Station 6, with the largest observation period, also has a notable difference between distribution choices at $T = 1000$, with the LN3 alternative resulting in the highest levels.

5. CONCLUDING REMARKS

In this paper, we have investigated the use of the Wakeby distribution. Through simulation studies, we found that based on several distance measures, the Wakeby distribution has a good fit to the tail, regardless of the distribution of origin (lognormal or generalised extreme-value distribution) and sample size. One could remark that although a certain distribution was registred as the "winner" (in terms of smallest distance), for a particular sample and choice of distance measure, often in practice the differences between distributions are quite small; cf. the detailed numerical outcomes for the flood data (Table 2).

In addition, we examined annual extreme floods with respect to fit of distribution and estimation of return levels. Uncertainties of return levels, e.g. in the form of confidence intervals, were not provided in the study, but although intervals in this context typically tend to be wide, the selection of the very distribution shows itself to be of interest for high quantiles ($T = 1000$).

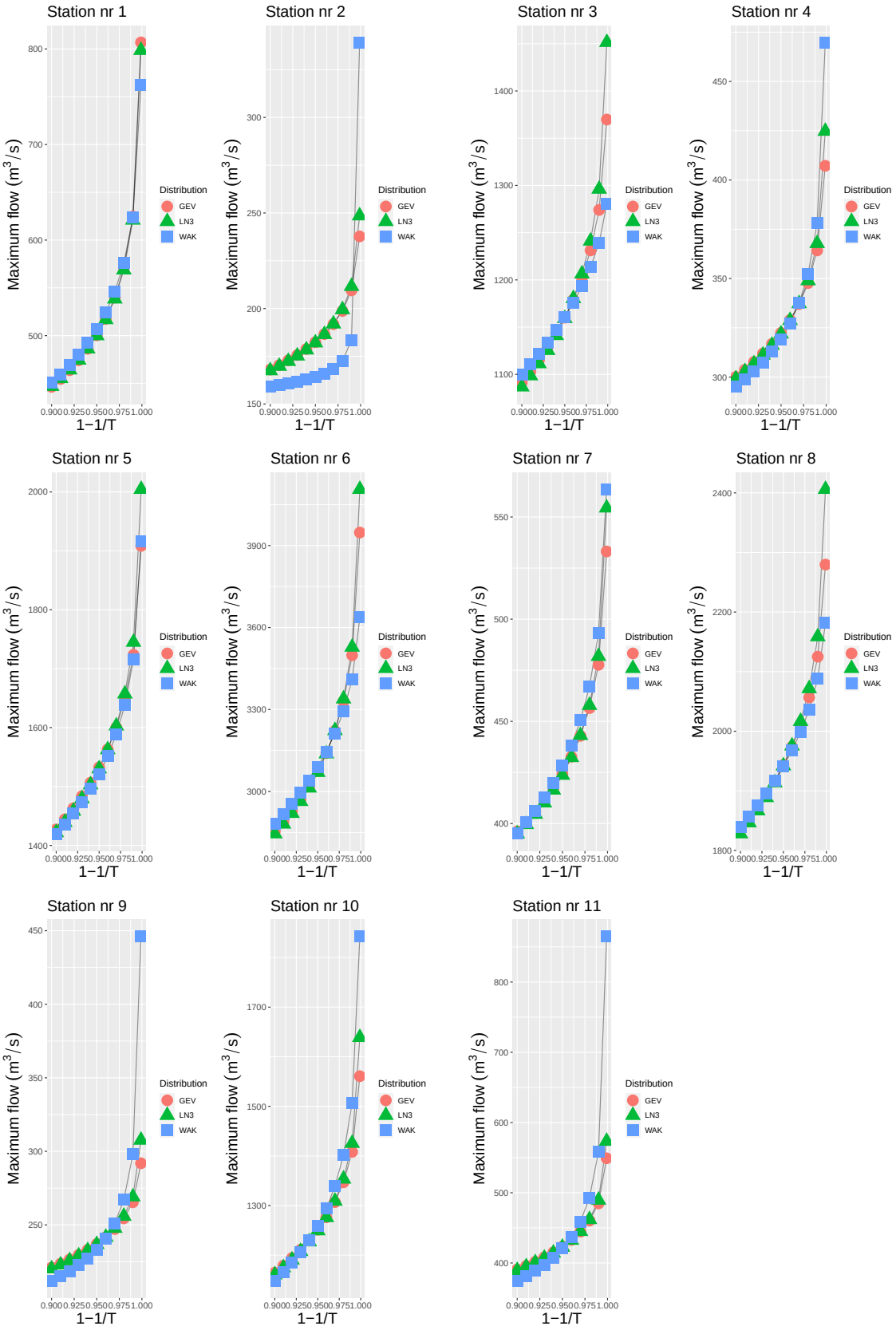

Figure 6: Return levels, based on station data. Abscissa: $1 - 1/T$, where T is the return period, starting from $T = 10$, final value $T = 1000$. The ordinate shows the related estimated return level.

We studied here the quantity of extreme floods, like in the vintage paper on Wakeby distribution [16]. In the literature, the Wakeby distribution has also been employed to model rainfall, [21] (although these authors did not motivate the choice of Wakeby distribution, compared to other alternatives). Further studies could be performed to investigate extreme rainfall. Moreover, concerning extreme daily rainfall, Papalexiou and Koutsoyiannis found by fitting GEV distributions to records worldwide that the record length strongly affects the estimate of the GEV shape [20]. Furthermore, the influence on the shape parameter was analysed. Further studies in this direction, employing a Bayesian approach are found in [24]. To conclude, the longer the observation series, the more likely the GEV distribution might be attained. Further studies on extreme floods with different observation lengths would be interesting.

Several options for analysis of minimum distance are available; for a review, see [8]. A version of the Anderson–Darling test statistic for analysis of tail deviation at the upper tail was suggested in [26]. The author experimented with that measure, but overall conclusions in the simulation studies were as for the measures presented in this paper: the Wakeby distribution gives the better fit.

To end this paragraph, and indeed the paper, we cite Haktanir and Horlacher [11]:

> "Because of the ample availability of computers nowadays, a single-site flood frequency analysis should be done with the inclusion of many standard probability distributions, and a final decision should be made combining experience with engineering judgement."

Even more today, some decades later, computers and related software are important tools. In a strategy for estimation for a certain region, one could still agree that several potential distributions are possible. Methodology for selection of candidates is of interest to further analyse.

APPENDIX

Let X be a real-valued random variable with distribution function $F(x)$ and quantile function $x(F)$. Moreover, denote by $X_{1:n} \le X_{2:n} \le X_{n:n}$ the order statistics for a random sample of size n. The L-moments are defined in [13] as the quantities

$$\lambda_r = \frac{1}{r}\sum_{k=0}^{r-1}(-1)^k\binom{r-1}{k}\mathsf{E}[X_{r-k:r}], \quad r = 1, 2, \ldots .$$

The first four L-moments can be shown to be

$$\begin{aligned}
\lambda_1 = \mathsf{E}[X] &= \int_0^1 x(F)\,\mathrm{d}F,\\
\lambda_2 = \mathsf{E}[X_{2:2} - X_{1:2}] &= \int_0^1 x(F)(2F-1)\,\mathrm{d}F,\\
\lambda_3 = \frac{1}{3}\mathsf{E}[X_{3:3} - 2X_{2:3} + X_{1:3}] &= \int_0^1 x(F)(6F^2-6F+1)\,\mathrm{d}F,\\
\lambda_4 = \frac{1}{4}\mathsf{E}[X_{4:4} - 3X_{3:4} + 3X_{2:4} - x_{1:4}] &= \int_0^1 x(F)(20F^3-30F^2+12F-1)\,\mathrm{d}F.
\end{aligned}$$

In practice, L-moments must be estimated from samples. The rth sample L-moment ℓ_r, estimated as a U-statistic, can be computed by

$$\ell_r = \frac{1}{n}\sum_{k=0}^{r-1}\sum_{i=1}^{n}(-1)^{r-1-k}\binom{r-1}{k}\binom{r-1+k}{k}\frac{(i-1)(i-2)\cdots(i-k)}{(n-1)(n-2)\cdots(n-k)}x_{i:n}.$$

Note, for instance, that $\ell_1 = \bar{x} = n^{-1}\sum_i x_i$.

L-moment ratios are L-moments that are standardized:

$$\tau_r = \frac{\lambda_r}{\lambda_2}, \quad r = 3, 4, \ldots .$$

Values of τ_3 and τ_4 are often plotted against each other, resulting in an L-moment diagram.

Hosking presents in [13], Table 1, the L-moment ratios for some common distributions. For instance, with relevance for this article, the Gumbel distribution has

$$\begin{aligned}
\tau_3 &= \ln(9/8)/\ln 2 \doteq 0.17,\\
\tau_4 &= (16\ln 2 - 10\ln 3)/\ln 2 \doteq 0.15.
\end{aligned}$$

For a GEV distribution with shape parameter ξ,

$$\begin{aligned}
\tau_3 &= 2(1-3)^{-\xi}/(1-2^{-\xi}) - 3,\\
\tau_4 &= \left[5(1-4^{-\xi}) - 10(1-3^{-\xi}) + 6(1-2^{-\xi})\right]/(1-2^{-\xi})
\end{aligned}$$

(the formula for τ_4 is here given following the report [12]; there seems to be a misprint in [13]).

ACKNOWLEDGMENTS

I am grateful to Staffan Betnér for discussion about visualisations and related coding. Thanks also to an anonymous referee for valuable comments.

REFERENCES

[1] Ahmad, U.N.; Shabri, A. and Zakaria, Z.A. (2011). Trimmed L-moments (1,0) for the generalized Pareto distribution, *Hydrological Sciences Journal*, **56**(6), 1053–1060.

[2] Akaike, H. (1974). A new look at the statistical model identification, *IEEE Transactions on Automatic Control*, **19**, 716–723.

[3] Anderson, T.W. and Darling, D.A. (1952). Asymptotic theory of certain "goodness-of-fit" criteria based on stochastic processes, *Annals of Mathematical Statistics*, **23**, 93–212.

[4] Arheimer, B. and Lindström, G. (2015). Climate impact on floods: changes in high flows in Sweden in the past and the future (1911–2100), *Hydrology and Earth System Sciences*, **19**, 771–784.

[5] Asquith, W. (2021). *lmomco – L-moments, censored L-moments, trimmed L-moments, L-comoments, and many distributions*, R package version 2.3.7.

[6] Aydoğan, D.; Kankal, M. and Önsoy, H. (2016). Regional flood frequency analysis for Çoruh Basin of Turkey with L-moments approach, *Journal of Flood Risk Management*, **9**(1), 69–86.

[7] Busababodhin, P.; Seo, Y.A.; Park, J.-S. and Kumphon, B. (2016). LH-moment estimation of Wakeby distribution with hydrological applications, *Stochastic Environmental Research and Risk Assessment*, **30**(6), 1757–1767.

[8] Cha, S.-H. (2007). Comprehensive survey on distance/similarity measures between probability density functions, *International Journal of Mathematical Models and Methods in Applied Sciences*, **4**(1), 300–307.

[9] Elamir, E.A.H. and Seheult, A.H. (2003). Trimmed L-moments, *Computational Statistics & Data Analysis*, **43**(3), 299–314.

[10] Griffiths, G.A. (1987). A theoretically based Wakeby distribution for annual flood series, *Hydrological Sciences Journal*, **34**(3), 231–248.

[11] Haktanir, T. and Horlacher, H.B. (1993). Evaluation of various distributions for flood frequency analysis, *Hydrological Sciences Journal*, **35**, 15–32.

[12] Hosking, J.R.M. (1986). *The theory of probability weighted moments*, "Research Report RC12210", IBM Research Division, Yorktown Heights, New York.

[13] Hosking, J.R.M. (1990). L-moments: analysis and estimation of distributions using linear combinations of order statistics, *Journal of the Royal Statistical Society, Series B*, **52**(1), 105–124.

[14] Hosking, J.R.M. (2019). *L-Moments*, R package, version 2.8.
`https://CRAN.R-project.org/package=lmom`

[15] Hosking, J.R.M. and Wallis, J.R. (1997). *Regional Frequency Analysis: An Approach Based on L-moments*, Cambridge University Press, Cambridge, United Kingdom.

[16] Houghton, J.C. (1978). Birth of a parent: the Wakeby distribution for modeling flood flows, *Water Resources Research*, **14**, 1105–1110.

[17] Jonsson, F. and Rydén, J. (2017). Statistical studies of the Beta Gumbel distribution: estimation of extreme levels of precipitation, *Statistica Applicata*, **29**, 5–27.

[18] Kullback, S. and Leibler, R.A. (1951). On information and sufficiency, *Annals of Mathematical Statistics*, **22**, 79–86.

[19] Önöz, B. and Bayazit, M. (1995). Best-fit distributions of largest available flood samples, *Journal of Hydrology*, **167**, 195–208.

[20] Papalexiou, S.M. and Koutsoyiannis, D. (2013). Battle of extreme value distributions: a global survey on extreme daily rainfall, *Water Resources Research*, **49**, 187–201.

[21] Park, J.-S.; Jung, H.-S.; Kim, R.-S. and Oh, J.-H. (2001). Modelling summer extreme rainfall over the Korean peninsula using Wakeby distribution, *International Journal of Climatology*, **21**, 1371–1384.

[22] Peel, M.C.; Wang, Q.J.; Vogel, R.M. and McMahon, T.A. (2001). The utility of L-moment ratio diagrams for selecting a regional probability distribution, *Hydrological Sciences – Journal des Sciences Hydrologiques*, **46**, 147–155.

[23] Persson, K. and Rydén, J. (2010). Exponentiated Gumbel distribution for estimation of return levels of significant wave height, *Journal of Environmental Statistics*, **1**(3), 1–12.

[24] Ragulina, G. and Reitan, T. (2017). Generalized extreme value shape parameter and its nature for extreme precipitation using long time series and the Bayesian approach, *Hydrological Sciences Journal*, **62**(6), 863–879.

[25] Schwarz, G.E. (1978). Estimating the dimension of a model, *Annals of Statistics*, **6**, 461–464.

[26] Shin, H.; Jung, Y.; Jeong, C. and Heo, J.-H. (2012). Assessment of modified Anderson-Darling test statistics for the generalized extreme value and generalized logistic distributions, *Stochastic Environmental Research and Risk Assessment*, **26**, 105–114.

[27] Šimková, T. and Picek, J. (2017). A comparison of L-, LQ-, TL-moment and maximum likelihood high quantile estimates of the GPD and GEV distribution, *Communications in Statistics – Simulation and Computation*, **46**(8), 5991–6010.

[28] Wilks, D.S. (1993). Comparison of three-parameter probability distributions for representing annual extreme and partial duration precipitation series, *Water Resources Research*, **29**, 3543–3549.